UNCLASSIFIED

AAEC/E 65

AAEC/E 65

AUSTRALIAN ATOMIC ENERGY COMMISSION
RESEARCH ESTABLISHMENT
LUCAS HEIGHTS

SEPARATING SMALL PARTICLES FROM LIQUIDS WITH THE HYDROCYCLONE

PART III – EFFECTS OF MAJOR OPERATING VARIABLES

by

E. G. THURSTAN

K. S. TURNER

Issued Sydney, July 1961

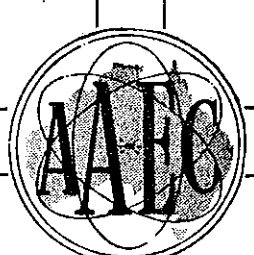

UNCLASSIFIED

AUSTRALIAN ATOMIC ENERGY COMMISSION

SEPARATING SMALL PARTICLES FROM LIQUIDS WITH THE HYDROCYCLONE

PART III – EFFECTS OF MAJOR OPERATING VARIABLES

by

E. G. THURSTAN

K. S. TURNER

ABSTRACT

For cyclone configurations producing flow ratios of 0.1 or less, the concentration efficiency increases as the feed concentration increases and then levels out at a concentration defined as the critical feed concentration. The clarification efficiency is independent of feed concentration up to concentrations slightly less than the critical feed concentration and then decreases. Both efficiencies increase logarithmically with flow rate. For a cyclone configuration of feed diameter (D_i) = 0.082 in., overflow diameter (D_o) = 0.098 in., and underflow diameter (D_u) = 0.037 in., correlations are proposed for the critical feed concentration in terms of the effective density ratio and concentration and clarification efficiencies in terms of the feed concentration, feed flow rate and the Rosin–Rammler–Bennett size distribution constant of the solid.

For cyclone configurations producing flow ratios from 0.2 to 0.5, the concentration efficiency is of minor importance. The clarification efficiency was found to be practically independent of concentration and also of flow rate except for materials with large distribution constants. Correlations are proposed for the clarification efficiency for a cyclone configuration of D_i = 0.055 in., D_o = 0.079 in., D_u = 0.058 in.

Optimum results may be obtained for a given suspension by choosing suitable flow ratios and hence cyclone configurations for each stage of a multi–stage unit. However, for maximum flexibility in handling changes in operating variables, a unit combining constant cyclone configuration with underflow throttling would be preferable.

The concentration and clarification efficiencies are not greatly affected by the average particle size or size distribution of the solid but the degree of classification obtained is markedly affected by both.

CONTENTS

(Continued)

CONTENTS (Continued)

1. INTRODUCTION

Small diameter hydrocyclones are envisaged as a convenient means of separating sub–sieve sized solids from liquids under radioactive conditions. For simultaneous concentration of solid and clarification of liquid, a two–stage unit is required, the first stage concentrating and the second clarifying (Trawinski, 1953). Part II of this work, by Cairns et al. (1961) on the effects of design variables on solids separation has established feed, overflow and underflow diameters for optimum concentration and maximum clarification for a hydrocyclone having a nominal diameter of 10 millimetres and treating an 11.5 ± 0.5 per cent. by weight suspension of sub–sieve barium sulphate in water. This report covers the work done to investigate the effects of major operating variables on solids separation.

Using six cyclone configurations, experimental data have been collected over a range of feed pressures (flow rates) and feed solid concentrations for aqueous suspensions of various solids and the results are given in this report.

Barium sulphate, red lead, talc, silica, titanium dioxide and zircon suspensions were circulated through cyclones having D_i = 0.082 in., D_o = 0.098 in., D_u = 0.037 in.; (chosen previously (Cairns et al., 1961) for optimum concentration) and D_i = 0.055 in., D_o = 0.079 in., D_u = 0.058 in.; (chosen previously (Cairns et al., 1961) for maximum clarification). Barium sulphate, red lead and zircon suspensions were also circulated through cyclones having D_i = 0.082 in., D_o = 0.157 in., D_u = 0.037 in., and D_i = 0.055 in., D_o = 0.060 in., D_u = 0.058 in. In addition, barium sulphate suspensions were circulated through cyclones having D_i = 0.082 in., D_o = 0.116 in., D_u = 0.037 in., and D_i = 0.055 in., D_o = 0.079 in., D_u = 0.037 in.

The solids used covered a wide range of densities and particle size distributions and were readily available in the sub–sieve size range.

2. APPARATUS AND METHOD

The experimental rig and method of collection of results were identical with those used previously (Cairns et al., 1961). For each combination of cyclone configuration and feed suspension used, runs were made at 10 (approximately), 20, 40 and 80 p.s.i.g. feed pressure. Feed solid concentrations varied from approximately 1 to 20 per cent. by weight for the barium sulphate, talc, and silica, from 2 to 30 per cent. for the red lead, and from 2 to 20 per cent. for the titanium dioxide and zircon.

The barium sulphate used was blanc fixe, manufactured by Farbenfabriken Bayer, A.G., of Germany and supplied by H.H. York and Co., of Sydney; the red lead was the "non–setting" grade supplied by Commonwealth Litharge and Red Lead Pty. Ltd., of Sydney; the talc was the T.S. pharmaceutical grade supplied by Austral Rock Milling Pty. Ltd., of Sydney. "Superfine" silica (ground quartz), "Tiona" brand ceramic grade anatase titanium dioxide and "milled" zircon were supplied by Ferro Corporation (Aust.) Pty. Ltd.

The physical properties of the solids, pertinent to this work are listed in Table 1. The cumulative particle size distributions were determined by the Sharples "Micromerograph". In a hydrocyclone high shear stresses are present (Trawinski, 1953) and deagglomeration of particles could be expected. As the Micromerograph gives the particle size distribution of a deagglomerated sample, it was considered that, compared with the available liquid sedimentation methods such as with the Andreasen pipette, the Micromerograph would most likely provide the particle size distribution effective within the cyclone. The particle size analyses given are means of results for samples taken before and during use and, for any one material, no significant differences between samples were found. Finite numerical values for the spread of particle sizes for each material were also obtained. This was done by plotting the Micromerograph results in Table 1 on a Rosin–Rammler–Bennett grid (Bennett, 1936) (log log per cent. by weight undersize versus log particle size) and determining the slopes of straight lines fitted to the points for each material. The values of the size distribution constant N thus obtained are included in Table 1.

Demineralised water was used for all suspensions. The temperature of the suspensions circulating during the experimental work varied between 32° and 41°C but did not vary by more than 2°C for any one combination of cyclone configuration and feed.

When using silica and zircon, erosion caused considerable enlargement of the underflow diameters, particularly the nominal 0.037 in. D_u, and frequent replacements were necessary. The nominal underflow diameters of 0.037 and 0.058 inches varied as follows:

	Before Use	After Use
Nominal 0.037 in.	0.036 in. to 0.040 in.	0.040 in. to 0.043 in.
	Except for zircon with the 0.082 in. D_i and the 0.157 in. D_o when the D_u varied from 0.033 in. to 0.035 in.	
Nominal 0.058 in.	0.054 in. to 0.058 in.	0.055 in. to 0.062 in.

When using a single hydrocyclone for solids separation, it has been customary to run the hydrocyclone to give the best compromise between concentration and clarification and, as the hydrocyclone is basically a classifier, to assess its performance by the use of separation curves in which efficiency is plotted against particle size.

To derive the separation curve the hydrocyclone is run with the feed and overflow diameters fixed and the underflow adjusted by trial and error to give the optimum compromise conditions just described. By using the correlations of Haas (1957), Bradley and Pulling (1959) or Matschke and Dahlstrom (1959), or by computation according to Matschke and Dahlstrom (1959), d_{50} (the particle size appearing 50 per cent. at both underflow and overflow) can be determined. By use of the Yoshioka and Hotta (1955) curve in which efficiency versus d/d_{50} is plotted, the separation curve can be obtained. On the premise that Stokes' law holds for particle motion within the cyclone, performance for other feed conditions can then be calculated. However, a change in feed concentration requires a change in underflow diameter to restore the optimum conditions followed by recalculation of d_{50} and of the separation curve. For design purposes this method of assessment is tedious and cumbersome.

Furthermore, it is considered that correlations involving d_{50} are of limited significance unless the particle size used is that effective within the cyclone. In some cases d_{50} correlations have been confirmed experimentally using for the particle diameters, Stokes' diameters determined by liquid sedimentation methods. However, different methods yield different results for the same material even though Stokes' diameters are measured in each case. Therefore, other means were chosen for assessment of hydrocyclone performance.

Cairns et al. (1959) discussed several expressions for efficiency. These included:

E_1, the solids elimination efficiency $= \frac{x_u w_u}{x_f w_f} \times 100$ (1)

E_2, the concentration efficiency $= \frac{x_u - x_f}{1 - x_f} \times 100$ (2)

and E_3, the clarification efficiency $= \frac{x_f - x_o}{x_f} \times 100$ (3)

where x_u = weight fraction of solids in the underflow stream,

w_u = underflow flow rate, g/sec,

x_f = weight fraction of solids in the feed stream,

w_f = feed flow rate, g/sec,

x_o = weight fraction of solids in the overflow stream.

During the work on the establishment of optimum dimensions (Cairns et al., 1961) the results were correlated in terms of the concentration and clarification efficiencies given by equations (2) and (3). In this work, the use of the concentration and clarification efficiencies was continued but better correlations were obtained by using volumetric efficiencies in which volume fractions of solids in the various streams were substituted for the corresponding weight fractions in equations (2) and (3).

Volumetric feed solid concentrations (C) were determined from the weight concentrations and the solid and liquid densities and for each run volumetric feed flow rates (VF) and volumetric efficiencies (E_2 and E_3) were determined. The calculations were done on an IBM 650 computer.

3. EFFECTS OF FEED CONCENTRATION AND FEED FLOW RATE

3.1 Using Cyclone I (0.082 in. D_i, 0.098 in. D_o, 0.037 in. D_u)

For each material, the results were first plotted on log–log paper as efficiency versus volumetric feed concentration with feed pressure as parameter. Typical results are shown in Figures 1 and 2 which give the results for talc and silica respectively. It can be seen that E_2 increases in direct proportion to C and then levels out at a feed concentration defined as the critical feed concentration (C_c). On the other hand E_3 is independent of C up to a feed concentration slightly less than the critical feed concentration and then decreases in approximately direct proportion to C.

It can also be seen from Figures 1 and 2 that feed pressure or flow rate variation causes a spread of the points for both E_2 and E_3 for each feed concentration and that the degree of spread depends on the suspended solid and whether C is greater or less than C_c. All the results were then plotted on log–log paper as efficiency versus volume flow rate. Although only approximate for the barium sulphate, straight lines were fitted to the points for each feed concentration for each material. Mean slopes (n) were obtained for both efficiencies (E_2 and E_3) for concentrations both greater and less than C_c. These are given in Table 2. Attempts were then made to correlate the results in terms of the physical properties of the solids.

3.1.1 Critical Feed Concentration

The critical feed concentration decreases with increase in solid density, so critical feed concentration was plotted against effective density ratio $\left(\frac{\rho_s-\rho_l}{\rho_l}\right)$ and the results are shown in Figure 3. The equation of the line in Figure 3 is

$$C_c = 7.9 \left(\frac{\rho_s-\rho_l}{\rho_l}\right)^{-0.56} \qquad (4)$$

which gives C_c in terms of the effective density ratio to within approximately 20 per cent. for solids with densities from 2.7 to 9.1 grams per cubic centimetre, having median Micromerograph particle sizes (δ) from 2.5 to 20 microns and Rosin–Rammler size distribution constants (N) from 1.4 to 2.9.

3.1.2 Concentration Efficiency

Figure 4 shows E_2 plotted against $C(VF)^n$ for the values of n given in Table 2 for feed concentrations less than the critical feed concentration. The flow rates corresponding to 10, 20, 40 and 80 p.s.i.g. feed pressures are approximately 19, 27, 37 and 51 ml per second for all materials except zircon. The corresponding flow rates for zircon are approximately 22, 31, 43 and 60 ml per second.

Figure 4 gives E_2 for a variety of materials for feed concentrations less than the critical feed concentration and for flow rates from approximately 20 to 50 ml per second. In general, the value of n increases (and the corresponding value of the intercept decreases) as the distribution constant N increases and an approximate correlation for n in terms of N was obtained by plotting n versus N on linear paper. This is shown in Figure 5, the equation of the line being

$$n = 0.3N - 0.33 \qquad (5)$$

For feed concentrations greater than C_c, the flow rates are approximately 10 per cent. greater than for those for feed concentrations less than C_c. E_2 is virtually independent of C within the limited range of C studied but still significantly affected by flow rate. Figure 6 gives a plot of E_2 versus $(VF)^n$ for the values of n given in Table 2 for feed concentrations greater than C_c. Again, in general, n increases as N increases and with the exception of the talc, equation (5) still gives the value of n to within approximately $\pm$ 0.1. However, further work is required to establish a correlation for n when the feed concentration is greater than the critical feed concentration.

3.1.3 Clarification Efficiency

For feed concentrations less than the critical feed concentration, E_3 was found to be independent of C but to vary as $(VF)^n$, where n is approximately 0.25 for the materials with the two largest size distribution constants and approximately 0.1 for the materials with the smaller values of N. Figure 7 shows the results plotted as E_3 versus $(VF)^n$ for these two values of n. For barium sulphate and talc, E_3 is given to within approximately 12 per cent. by

$$E_3 = 30(VF)^{0.25} \qquad (6)$$

For silica, zircon, titanium dioxide and red lead, E_3 is given to within approximately 6 per cent. by

$$E_3 = 59(VF)^{0.1} \qquad (7)$$

For feed concentrations greater than C_c, E_3 showed a greater variation with feed pressure than for feed concentrations less than C_c and also decreased with increase in C. A satisfactory correlation could not be obtained for feed concentrations greater than C_c.

The results in Figures 1 and 2 show that E_2 usually increases with increase in feed pressure (flow rate) but for some of the 80 p.s.i.g. runs for silica, E_2 shows a definite decrease. A decrease was also obtained for some of the 80 p.s.i.g. runs for red lead and zircon. It appears that at high flow rates in this cyclone some change in the flow pattern within the cyclone may occur and the abnormal results were omitted in the subsequent calculations for both E_2 and E_3.

3.2 Using Cyclone II (0.055 in. D_i, 0.079 in. D_o, 0.058 in. D_u).

The results were plotted as in Figures 1 and 2 and those for titanium dioxide and red lead shown in Figures 8 and 9, are typical. For this cyclone the flow rates corresponding to 10, 20, 40 and 80 p.s.i.g. feed pressures are approximately 10, 14, 20 and 28 ml per second.

3.2.1 Concentration Efficiency

As for cyclone I, E_2 was still directly proportional to C and variation in flow rate had a greater effect on efficiency for solids with the larger size distribution constants than for those with the smaller values of N. A similar increase of n with N was obtained but the values of n for cyclone II were somewhat lower than the corresponding values for cyclone I. For corresponding feed concentrations and feed flow rates, the values of E_2 for cyclone II were much lower than those for cyclone I. For a multi–stage unit configuration II would not therefore be considered for the first stage and in any later stage, the underflow stream normally would be recycled so the concentration efficiency for configuration II is of minor importance.

3.2.2 Clarification Efficiency

For the minimum feed pressure runs for barium sulphate, E_3 decreased slightly with increase in C for values of C greater than approximately 2 per cent. Similar results were obtained for talc for values of C greater than approximately 5 per cent. but, in general, E_3 was found to be independent of C. The values of E_3 for cyclone II are similar to those obtained for feed concentrations less than C_c in cyclone I but for cyclone II they were obtained at lower flow rates. The mean slopes of efficiency versus flow rate plots are given in Table 3 and again it can be seen that there is a significant difference between the results for the materials with the two largest size distribution constants and those with the smaller values of N. Ignoring the minimum feed pressure results for $C > 2$ per cent. for barium sulphate and $C > 5$ per cent. for talc it was found that for these materials E_3 is given to within approximately 8 per cent. by

$$E_3 = 37(VF)^{0.25} \qquad (8)$$

For the other materials, similar values of E_3 are obtained for all feed concentrations and the variation of E_3 with flow rate is practically insignificant. The results were therefore correlated by taking a mean value of E_3 for all feed concentrations and flow rates. The mean value was 84 per cent. and all the results for silica, zircon, titanium dioxide and red lead were within approximately 11 per cent. of this figure.

3.3 Using Other Cyclone Configurations

During the previous work on an 11.5 per cent. by weight suspension of barium sulphate (Cairns et al., 1961), it was found that both E_2 and E_3 were affected by changes in each of the feed, overflow and underflow diameters but that, in general, configurations producing the same flow ratio gave similar results. In view of this, the effects of feed concentration and feed flow rate for other cyclone dimensions were investigated by using cyclone configurations chosen to produce a range of flow ratios. The flow ratios for the optimum concentration and maximum clarification configurations were 0.1 and 0.4 respectively and results were obtained for barium sulphate suspensions for cyclones producing flow ratios of 0.03 to 0.5. In addition to cyclones I and II, cyclones III (0.082 in. D_i, 0.157 in. D_o, 0.037 in. D_u, 0.03 R_f), IV (0.082 in. D_i, 0.116 in. D_o, 0.037 in. D_u, 0.06 R_f), V(0.055 in. D_i, 0.079 in. D_o, 0.037 in. D_u, 0.2 R_f) and VI (0.055 in. D_i, 0.060 in. D_o, 0.058 in. D_u, 0.5 R_f) were used. Figures 10 to 15 show the results for barium sulphate for cyclones III, IV, I, V, II and VI respectively. Red lead and zircon suspensions also were circulated through cyclones III and VI and the results supported the results obtained with the barium sulphate. The flow rates shown in Figures 10 to 15 are means for all feed concentrations used at the indicated feed pressure.

The results for cyclones III and IV show a similar pattern to those for cyclone I. E_2 increases with increase in C and then levels out but at concentrations lower than those obtained with cyclone I. The critical feed concentration is much less sharply defined for the smaller flow ratios but, for a flow ratio of 0.03, the critical feed concentration is approximately half of that for a flow ratio of 0.1. The value of E_2 at the critical feed concentration is approximately the same as that for cyclone I. Hence, for a given feed concentration less than the critical feed concentration for cyclone III, higher values of E_2 are obtained for cyclones III and IV than for cyclone I. However corresponding values of E_3 are lower, particularly for low flow rates, due to the greater variation of efficiency with flow rate.

Cyclone VI results are similar to those for cyclone II except that corresponding values of E_2 are slightly lower.

The results for cyclone V are intermediate between those for cyclones I and II in that there is evidence of a critical feed concentration but the values at which E_2 levels out are lower than the corresponding values of E_2 using cyclone I.

It can be seen from the results in Figures 10 to 15 that, for a given feed suspension, it is desirable to select a suitable flow ratio for each stage of a multi-stage unit and that a change in feed concentration (or feed solid) would require a change of flow ratio(s) and hence change of cyclone dimensions

to maintain optimum operation. The order of results that could be expected is shown in Table 4, which is compiled from most of the data in Figures 10 to 15.

A more convenient method of changing the flow ratio which, in effect, changes the underflow diameter is to throttle the underflow stream after it leaves the cyclone. Hence by selecting for all stages a cyclone configuration which would normally give a large flow ratio and hence high clarification efficiencies for a wide range of feed conditions, high underflow concentrations from the first stage may be maintained for a range of feed concentrations and feed solids by controlling the underflow flow rate. This method also has the advantage of minimising the effects of erosion. The technique of constant cyclone configuration combined with underflow throttling is used in practice as, for example, in the Dorrco TM unit (Dorr–Oliver Inc., 1953).

During the earlier work on barium sulphate, it was found that similar flow ratios were obtained for similar ratios of D_o/D_u. Hence by increasing D_u of cyclone I to $\frac{D_c}{4}$, a similar flow ratio and hence similar results to those for cyclone VI could be expected. It is interesting to note that such a cyclone configuration

$$(D_i = \frac{D_c}{5},\ D_o = \frac{D_c}{4},\ D_u = \frac{D_c}{4})$$

is very similar to the Dorrco configuration (Dorr–Oliver N.V., 1955)

$$(D_i = D_o = D_u = \frac{D_c}{4})$$

for a 10 millimetre cyclone.

4. EFFECT OF FEED SOLID PARTICLE SIZE

As feed particle size affects hydrocyclone performance, it was necessary to investigate the effect of particle size distribution on E_2 and E_3. This requires choice of a method for particle size measurement, which yields the particle size distribution effective within the hydrocyclone and a simple method of mathematically defining the particle size distribution. Previous work had shown that the Andreasen liquid sedimentation method was unsuitable and the Micromerograph gas sedimentation method was chosen for the reasons given in Section 2.

Finite figures for average size and size spread can be obtained, if a straight line on suitable co–ordinates represents the particle size distribution. The Micromerograph particle size distributions of all the feed solids used were found to give the best straight line plots on a Rosin–Rammler–Bennett grid. Even though this may not apply generally to all materials,this method of representation of size distribution is considered justified, particularly as the materials used were chosen at random within the subseive range.

It was not possible to circulate different particle size distributions of the same solid but from the results already given it can be seen, for the range of particle size distributions studied, that E_2 and E_3 are apparently unaffected by the average particle size of the feed solid represented by the median or 50 per cent. by weight undersize value (δ) but that the spread of sizes has some effect by its influence on the efficiency versus flow rate relationships. On the other hand the effect of δ and N on the degree of classification obtained is considerable.

Kelsall (1952) has pointed out that there is a conical envelope of zero vertical velocity within a cyclone and all particles within this envelope are removed via the overflow and all outside it are removed via the underflow. As a result of the opposing centrifugal and radial forces particles tend to move to equilibrium positions and form envelopes of constant particle size, concentric with the cyclone wall. Equilibrium envelopes for the smallest sizes are near the cyclone axis within the envelope of zero vertical velocity and those for the largest sizes are near the cyclone wall outside

the envelope of zero vertical velocity. Provided that the particles have sufficient time to reach their equilibrium positions, the smaller particles are discharged at the overflow and the larger particles at the underflow and hence classification occurs. However, Kelsall also pointed out that the equilibrium envelopes are bands of finite width due to turbulence and hence as the mean particle size and size range of the feed solid are reduced a decrease in the degree of classification as indicated by the difference between underflow and overflow size distributions could be expected. This was confirmed.

For the runs shown in Table 5, Micromerograph particle size distributions were determined for feed, underflow and overflow solids. Typical results are shown in Table 6.

For red lead (δ = 2.5, N = 2.5) and barium sulphate (δ = 3.8, N = 2.7), there is no difference between underflow and overflow size distributions. For titanium dioxide (δ = 7.9, N = 2.0), there is a small but insignificant difference and for talc (δ = 15, N = 2.9), silica (δ = 14, N = 1.4) and zircon (δ = 19, N = 1.5) progressively larger differences are obtained. It is obvious that the degree of classification increases with both increase in mean particle size and with decrease in size distribution constant but it should be noted that the degree of classification has little effect on the concentration or clarification efficiencies. This can be seen by comparing for example the results for barium sulphate and silica. From Figures 12 and 2, for C = 1 per cent. feed pressure = 20 p.s.i.g. values of 5.9 per cent. and 5.6 per cent. for E_2 and values 74 per cent. and 81 per cent. for E_3 were obtained for the barium sulphate and silica respectively although the difference in the degree of classification as shown by the difference in particle size distributions given in Table 6 is quite marked.

5. CONCLUSIONS

(i) The effects of feed concentration and feed flow rate on the concentration and clarification efficiencies depend on the cyclone configuration and the properties of the feed solid.

(ii) For a cyclone configuration of 0.082 in. D_i, 0.098 in. D_o, 0.037 in. D_u, corresponding to a flow ratio of 0.1, E_2 increases with increase in C and then levels out at a concentration defined as the critical feed concentration (C_c). E_3 is independent of C up to a concentration slightly less than C_c and then decreases with increase in feed concentration. Both E_2 and E_3 increase with increase in VF for all concentrations.

For feed concentrations less than C_c, E_2 can be obtained from Figure 4 in which E_2 is plotted against $C(VF)^n$. The value of n depends on the feed solid and an approximate correlation for n in terms of the size distribution constant N is given by

$$n = 0.3N - 0.33$$

For barium sulphate and talc which had the two largest values of N, E_3 is given by

$$E_3 = 30(VF)^{0.25}$$

For silica, zircon, titanium dioxide and red lead which had the lower values of N,

$$E_3 = 59(VF)^{0.1}$$

For feed concentrations greater than C_c, E_2 varies as $(VF)^n$ where n again appears to be a function of N, but further work is required to establish a correlation for n for the higher feed concentrations. Further work is also required to establish a correlation for E_3 for the higher feed concentrations.

The critical feed concentration decreases with increase in solid density and is given in terms of the effective density ratio by

$$C_c = 7.9 \left(\frac{\rho_s - \rho_l}{\rho_l}\right)^{-0.56}$$

(iii) For a cyclone configuration of 0.055 in. D_i, 0.079 in. D_o, 0.058 in. D_u, corresponding to a flow ratio of 0.4, E_3 is virtually independent of C for all materials. For the materials with the two largest values of N, E_3 is given by

$$E_3 = 37(VF)^{0.25}$$

For other materials E_3 is also practically independent of VF and is given by the mean figure of 84 per cent.

For this configuration, E_2 is of minor importance.

(iv) For cyclone configurations producing flow ratios of less than 0.1, lower values of the critical feed concentration are obtained and for a feed concentration less than the critical feed concentration for a given cyclone, higher values of E_2 are obtained for the lower flow ratios than for the corresponding feed concentration at a flow ratio of 0.1. However corresponding values of E_3 are lower, particularly for low flow rates, due to the greater variation of efficiency with flow rate.

(v) For cyclone configurations producing flow ratios of 0.2 to 0.5, no well defined critical feed concentration was found. For corresponding feed concentrations E_2 steadily decreases and high values of E_3 are maintained for all feed concentrations within the concentration range studied.

(vi) For optimum results with a given suspension, cyclones for each stage should be individually designed. For flexibility in handling changes in feed solids and feed concentration, the combination of constant cyclone configuration with underflow throttling would be more satisfactory.

(vii) Both average particle size and particle size distribution have a considerable effect on the degree of classification obtained but the concentration and clarification efficiencies are only slightly affected.

(viii) Further work is required to confirm the proposed relationships, particularly for higher feed concentrations and trial runs should be made on new suspensions.

(ix) Further work is required on the effect of liquid viscosity.

6. ACKNOWLEDGMENTS

Acknowledgments are due to Mr. C. L.W. Berglin for his helpful advice and Mr. J.R. May who provided most of the Micromerograph results.

7. SYMBOLS

C = feed solid concentration (per cent. by volume)

C_c = critical feed concentration (per cent. by volume)

D_c = cyclone diameter (in)

D_i = feed diameter (in)

D_o = overflow diameter (in)

D_u = underflow diameter (in)

E_1 = solids elimination efficiency (per cent.)

E_2 = concentration efficiency (per cent.)

E_3 = clarification efficiency (per cent.)

n = flow rate exponent in correlations for efficiency

N = size distribution constant

R_f = flow ratio = underflow volumetric flow rate / feed volumetric flow rate

VF = feed flow rate (ml/sec)

w_f = feed flow rate (g/sec)

w_u = underflow flow rate (g/sec)

x_f = weight fraction of solids in the feed stream

x_o = weight fraction of solids in the overflow stream

x_u = weight fraction of solids in the underflow stream

δ = median, or 50 per cent. by weight undersize particle diameter,(microns)

ρ_l = density of liquid (g/cc)

ρ_s = density of solid (g/cc)

8. REFERENCES

Bennett, J.G., 1936. J. Inst. Fuel, 10 : 22.

Bradley, D. and Pulling, D.J., 1959. Trans. Instn. Chem. Engrs., 37 : 34.

Cairns, R.C., Thurstan, E.G. and Turner, K.S., 1959. AAEC/E 45.

Cairns, R.C., Thurstan, E.G. and Turner, K.S., 1961. AAEC/E 63.

Dorr–Oliver Incorporated, 1953. Bulletin No. 2502.

Dorr–Oliver, N.V., 1955. Operating Instructions for TM1 Dorrclone. Dorr–Oliver N.V. Amsterdam.

Haas, P.A., 1957. U.S.A.E.C. Report ORNL 2301.

Kelsall, D.F., 1952. Trans.Instn. Chem. Engrs, 30 : 87.

Matschke, D.E. and Dahlstrom, D.A., 1959. C.E.P., 55 : 79.

Trawinski, H., 1953. A.E.R.E. Lib./Trans. 605 from Chemie. – Ingenieur Technik. 25 : 331.

Yoshioka, N. and Hotta, Y., 1955. A.E.C. Tr. 2476 from Chemical Engineering Japan, 19 : 632.

TABLE 1

Properties of Solids Used

Property	Material											
	Barium Sulphate		Red Lead		Talc		Silica		Titanium Dioxide		Zircon	
	wt. % under–size	microns	wt. % under–size	microns	wt. % under–size	microns	wt. % under–size	microns	wt. % under–size	microns	wt. % under–size	microns
Micromerograph Particle Size Distribution	100	17	100	8.8	100	44	100	64	100	27	100	67
	90	6.7	90	4.6	90	25	90	41	90	15	90	42
	80	5.4	80	3.8	80	22	80	30	80	12	80	34
	70	4.7	70	3.2	70	19	70	24	70	10	70	28
	60	4.2	60	2.8	60	17	60	18	60	8.9	60	23
	50	3.8	50	2.5	50	15	50	14	50	7.9	50	19
	40	3.4	40	2.2	40	13	40	11	40	6.8	40	16
	30	3.0	30	2.0	30	12	30	8.2	30	5.7	30	12
	20	2.5	20	1.7	20	10	20	6.0	20	4.4	20	8.5
	10	2.1	10	1.4	10	7.4	10	3.8	10	3.1	10	5.6
	0	1.4	0	1.0	0	2.7	0	1.6	0	1.6	0	2.2
Rosin–Rammler–Bennett Size Distribution Constant (N)	2.7		2.5		2.9		1.4		2.0		1.5	
Density (ρ_s) g/cc	4.5		9.1		2.7		2.7		3.8		4.7	

NOTE: The values of N quoted were obtained from the Micromerograph undersize values of 10 per cent. to 90 per cent. inclusive.

TABLE 2

Slopes of Efficiency Versus Flow Rate Plots for Cyclone I

	Silica		Zircon		Titanium Dioxide		Red Lead		Barium Sulphate		Talc	
	E_2	E_3	E_2	E_3	E_2	E_3	E_2	E_3	E_2	E_3	E_2	E_3
$C < C_c$	0.21	0.09	0.03	0.08	0.23	0.12	0.28	0.06	0.58	0.30	0.56	0.23
$C > C_c$	0.23	0.39	0.13	0.19	0.24	0.32	0.44	0.24	0.54	0.47	0.29	0.31

NOTE: Results for concentrations coinciding with the critical concentration are included with those for concentrations greater than the critical concentration.

TABLE 3

Slopes of Efficiency Versus Flow Rate Plots for Cyclone II

	Silica	Zircon	Titanium Dioxide	Red Lead	Barium Sulphate	Talc
E_2	0.06	−0.10	0.11	0.09	0.26	0.32
E_3	0.06	0	0.11	0.07	0.26	0.27

TABLE 4

Underflow and Overflow Concentrations for Various Cyclone Combinations

Initial Feed Conc.	Initial Feed Flow Rate	1st Stage Underflow Conc.		2nd Stage Overflow Conc.			
		$R_f = 0.03$ (Cyclone III)	$R_f = 0.1$ (Cyclone I)	$R_f = 0.1$ (Cyclone I)	$R_f = 0.2$ (Cyclone V)	$R_f = 0.4$ (Cyclone II)	$R_f = 0.5$ (Cyclone VI)
Vol. %	ml/sec	Vol. %	Vol. %	Vol. %	Vol. %	Vol. %	Vol. %
0.23	28	2.86		–	–	–	–
0.50	28	6.10		0.08	0.04	0.06	0.06
0.97	28	10.9		0.16	0.09	0.11	0.11
1.98	28	16.1		0.38	0.21	0.26	0.22
2.89	28	19.4		0.68	0.34	0.39	0.32
4.12	28	20.9		1.7	0.59	0.59	0.45
5.38	28	22.4		2.8	1.3	0.79	–
0.23	22		1.34	–	–	–	–
0.46	22		2.76	–	–	–	–
0.89	22		5.54	0.10	0.05	0.06	0.06
1.90	22		11.6	0.22	0.11	0.15	0.13
2.81	22		16.3	0.47	0.24	0.30	0.27
4.15	22		20.4	1.2	0.50	0.55	0.48
5.52	22		21.4	2.3	1.2	0.84	0.69

NOTE: 1. The gaps in columns 5 to 8 are due to the omission of data requiring extrapolation of experimental results.

2. The results in column 3 are means of the experimental results obtained for the minimum feed pressure (8 p.s.i.g. 22 ml/sec) and the 20 p.s.i.g. (34 ml/sec) runs in Figure 10.

3. The results in column 4 are means of the experimental results obtained for the minimum feed pressure (8 p.s.i.g. 18 ml/sec) and the 20 p.s.i.g. (27 ml/sec) runs in Figure 12.

4. The results in columns 5 to 8 were calculated from values of E_3 taken from Figures 12 to 15 respectively. The feed flow rates used to obtain E_3 were calculated from the initial feed flow rates and the 1st stage flow ratio. The feed concentrations used to obtain E_3 were the overflow concentrations corresponding to the results in columns 3 and 4.

TABLE 5

Particle Size Analysis Samples

Cyclone	Material and Feed Concentration (approximate wt. %)					
	Barium Sulphate	Red Lead	Talc	Silica	Titanium Dioxide	Zircon
I	2, 12	16	8, 12, 20	8, 12, 20	8, 20	8, 12, 20
II	12		4	4	4	4
III	20	16				
VI		4				12

NOTE: Feed Pressure 20 p.s.i.g. in all cases.

TABLE 6

Particle Size Analyses for Various Conditions

Material and Conditions	Stream	Particle Diameter in microns, for										
		100	90	80	70	60	50	40	30	20	10	0
		wt. % undersize										
Barium Sulphate, Cyclone II, 12 wt. % Feed conc., 20 p.s.i.g. Feed press.	Feed	18	6.9	5.5	4.8	4.4	3.9	3.5	3.0	2.5	2.1	1.4
	Underflow	31	6.9	5.5	4.7	4.2	3.8	3.4	3.0	2.6	2.1	1.4
	Overflow	31	6.5	5.2	4.5	4.0	3.6	3.2	2.8	2.4	1.9	1.4
Red Lead, Cyclone III, 16 wt. % Feed conc., 20 p.s.i.g. Feed press.	Feed	10	4.9	3.8	3.3	2.8	2.5	2.2	2.0	1.7	1.4	1.0
	Underflow	10	5.1	4.2	3.6	3.2	2.8	2.5	2.1	1.8	1.4	1.0
	Overflow	10	4.6	3.7	3.1	2.7	2.4	2.2	2.0	1.7	1.4	1.0
Talc, Cyclone I, 8 wt. % Feed conc., 20 p.s.i.g. Feed press.	Feed	29	23	20	18	16	14	13	11	9.4	7.1	3.0
	Underflow	33	24	22	20	19	17	15	13	11	8.4	3.0
	Overflow	26	17	15	14	12	11	10	8.9	7.5	6.0	3.0
Silica, Cyclone I, 12 wt. % Feed conc., 20 p.s.i.g. Feed press.	Feed	55	40	30	23	18	14	11	8.5	6.4	4.3	1.8
	Underflow	74	41	32	26	21	17	13	11	8.3	5.9	2.4
	Overflow	16	9.2	7.5	6.4	5.7	5.0	4.3	3.7	3.1	2.4	1.5
Titanium Dioxide Cyclone I, 8 wt. % Feed conc., 20 p.s.i.g. Feed press.	Feed	28	15	12	10	9.0	7.9	6.8	5.5	4.3	3.0	1.6
	Underflow	22	14	11	9.8	8.8	7.8	6.8	5.9	4.8	3.3	1.6
	Overflow	28	12	10	9.0	7.7	6.6	5.5	4.4	3.4	2.5	1.6
Zircon Cyclone VI, 12 wt. % Feed conc., 20 p.s.i.g. Feed press.	Feed	–	41	32	25	20	17	13	10	7.1	4.5	1.4
	Underflow	86	46	36	29	24	20	16	13	9.5	6.3	1.9
	Overflow	20	10	8.4	7.1	6.2	5.3	4.6	3.9	3.1	2.4	–

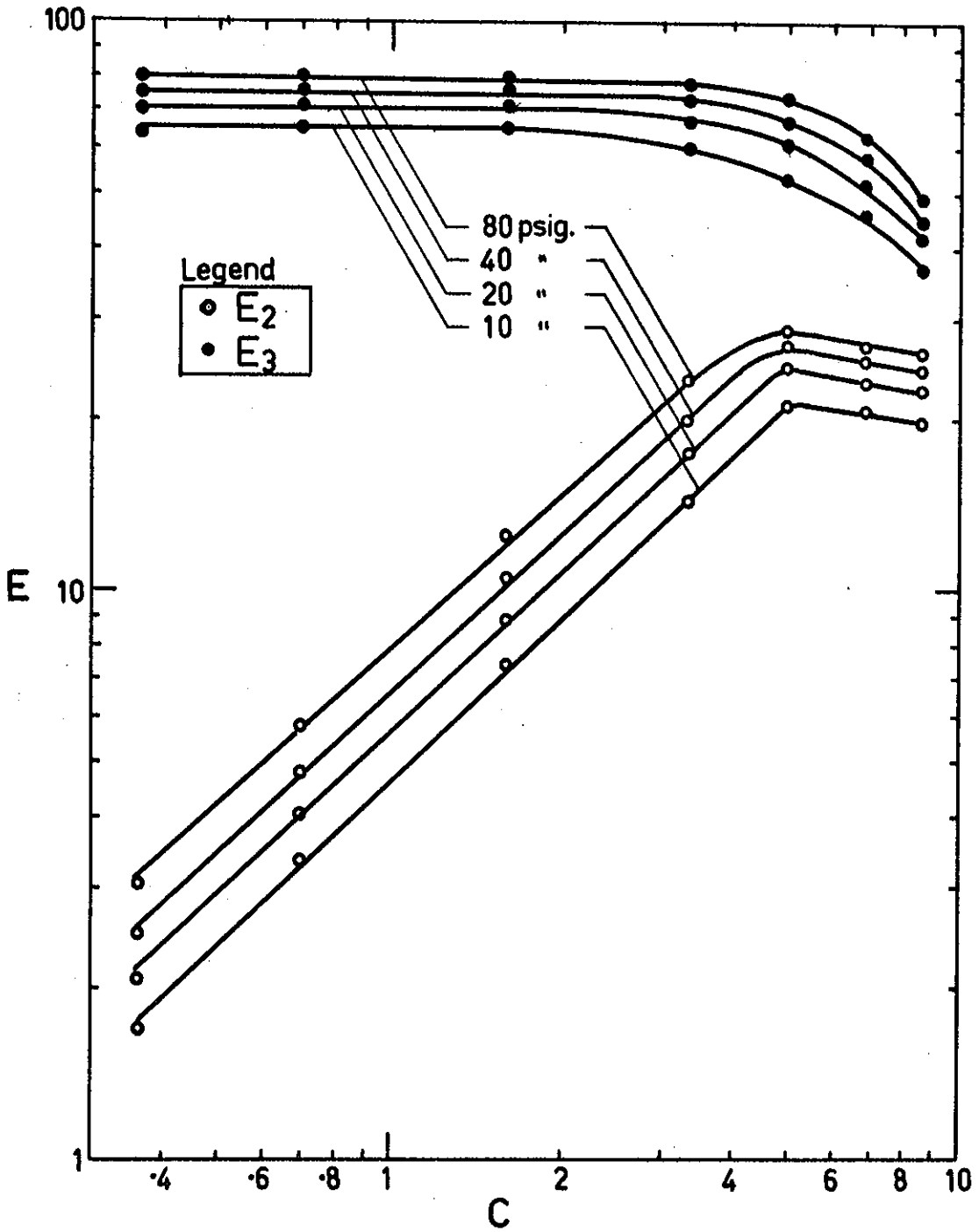

FIG. 1 EFFICIENCY vs. FEED CONCENTRATION FOR TALC – CYCLONE I

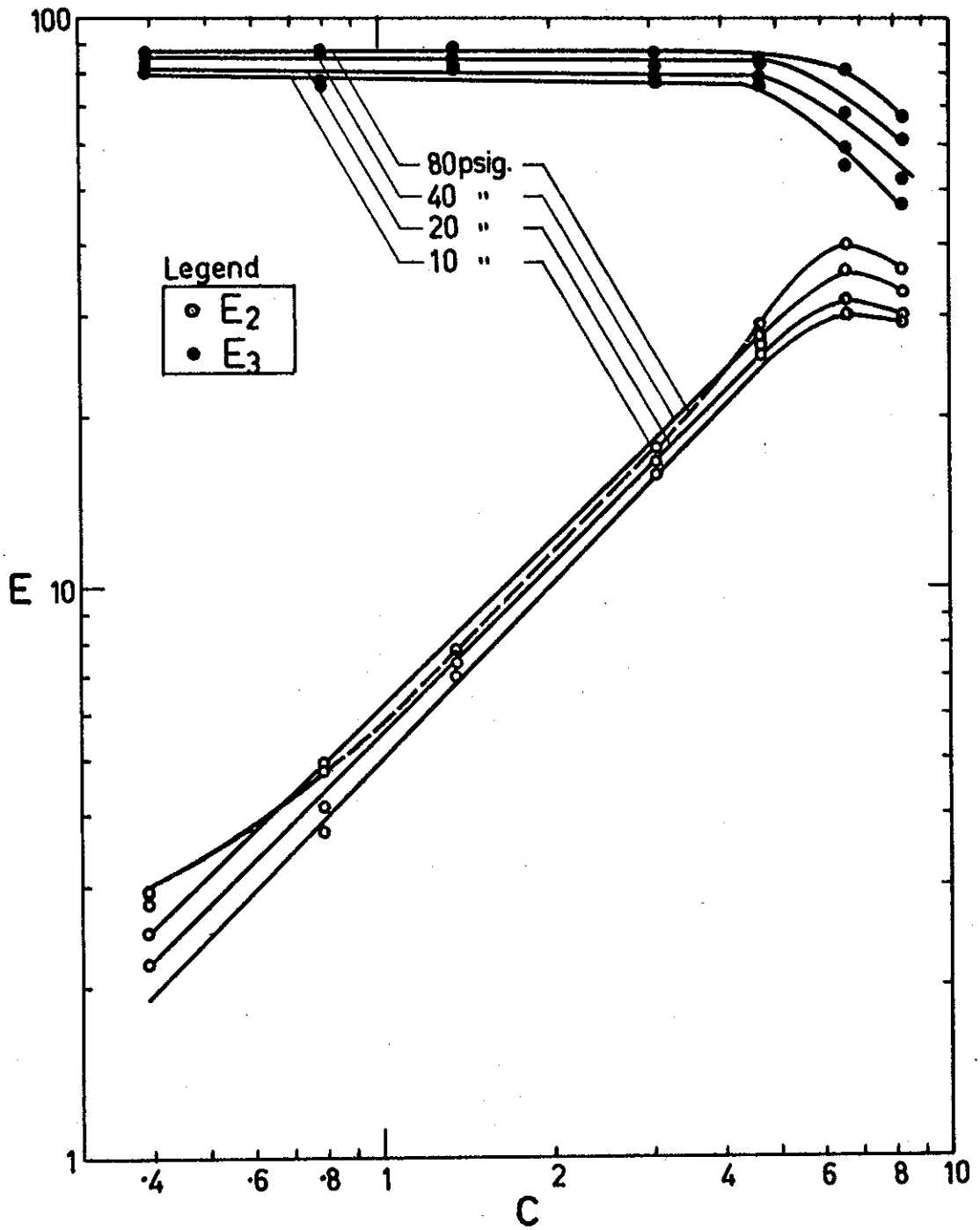

FIG. 2 EFFICIENCY vs. FEED CONCENTRATION FOR SILICA – CYCLONE I

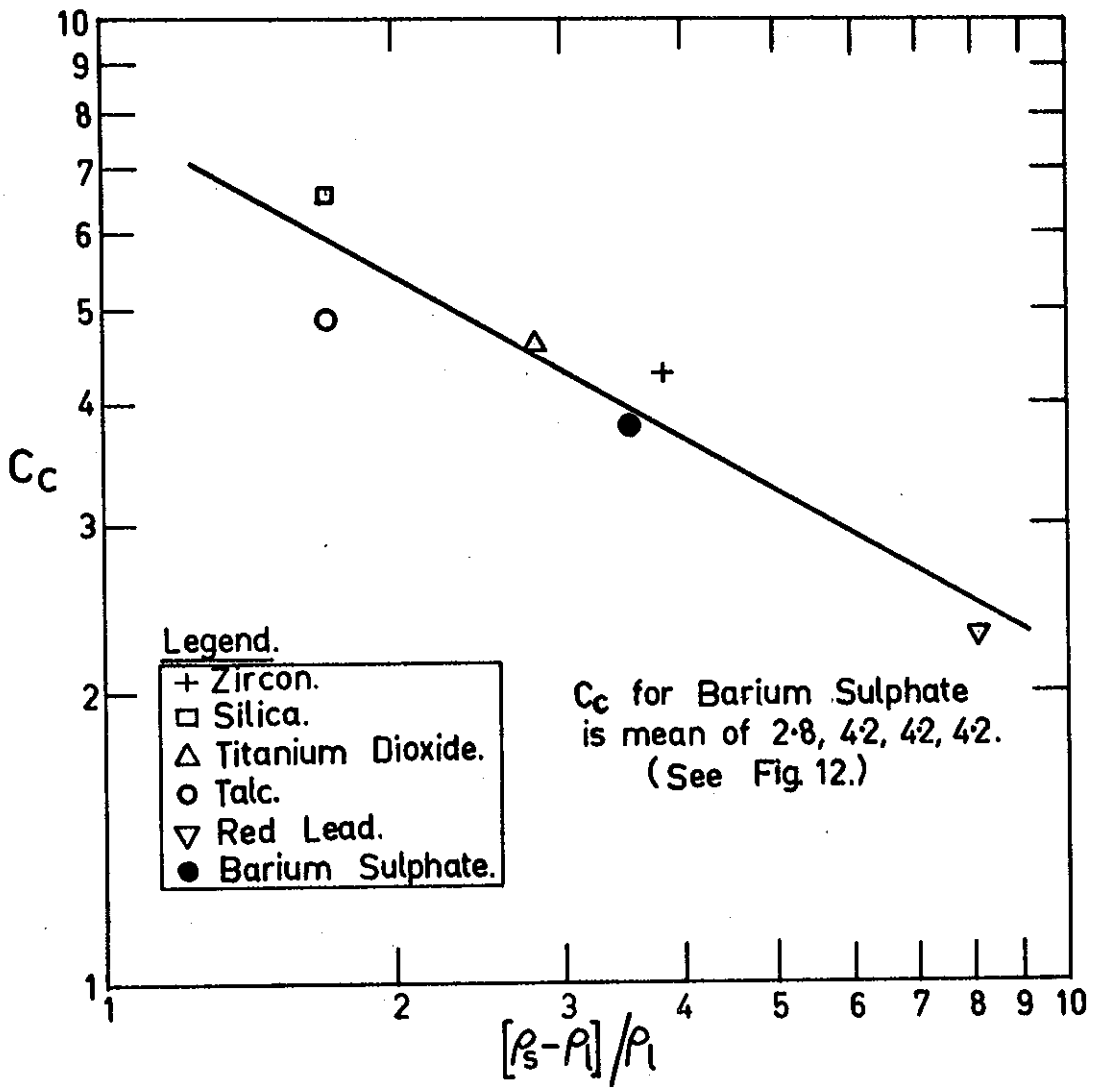

FIG. 3 CRITICAL FEED CONCENTRATION vs. EFFECTIVE DENSITY RATIO.- CYCLONE I

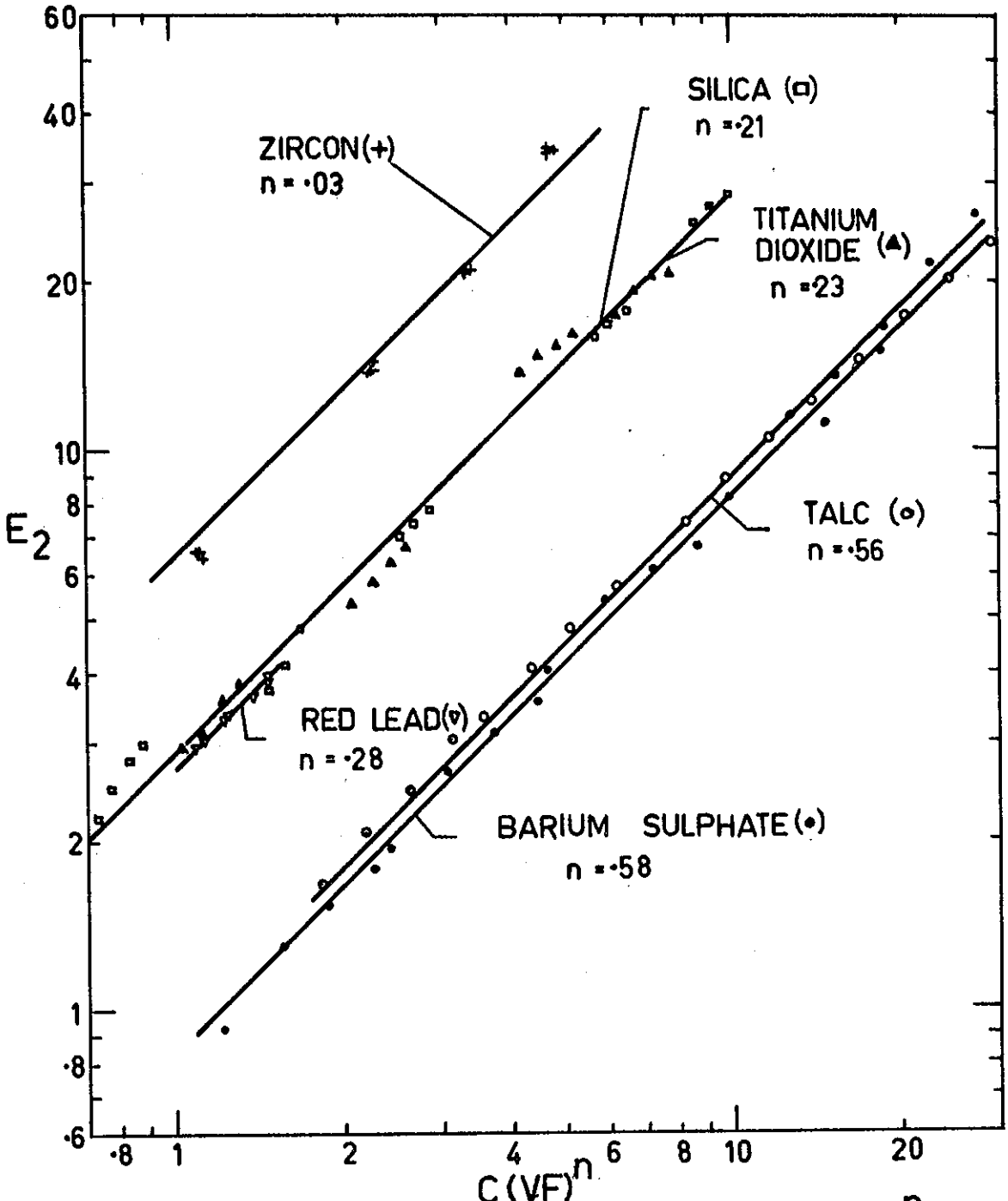

FIG. 4 CONCENTRATION EFFICIENCY vs. $C(VF)^n$ FOR $C < C_c$ – CYCLONE I

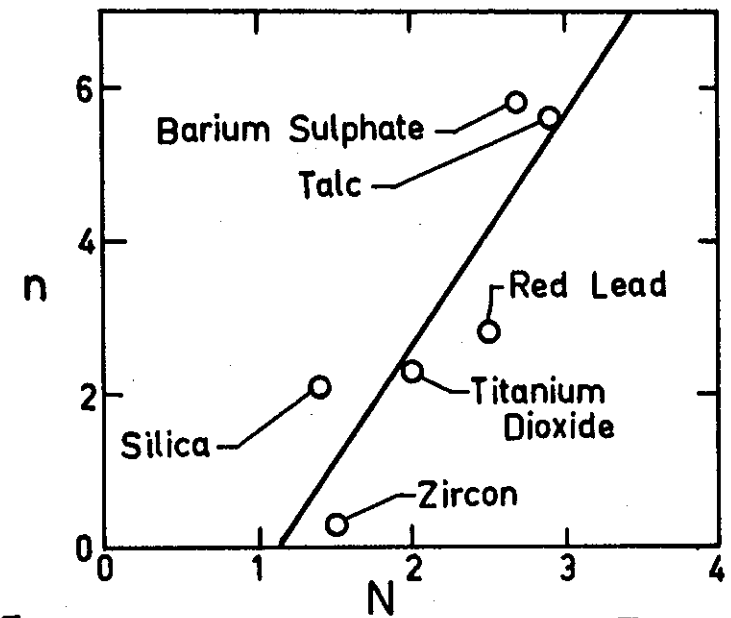

FIG. 5 FLOW RATE EXPONENT OF FIG. 4 vs. SIZE DISTRIBUTION CONSTANT.

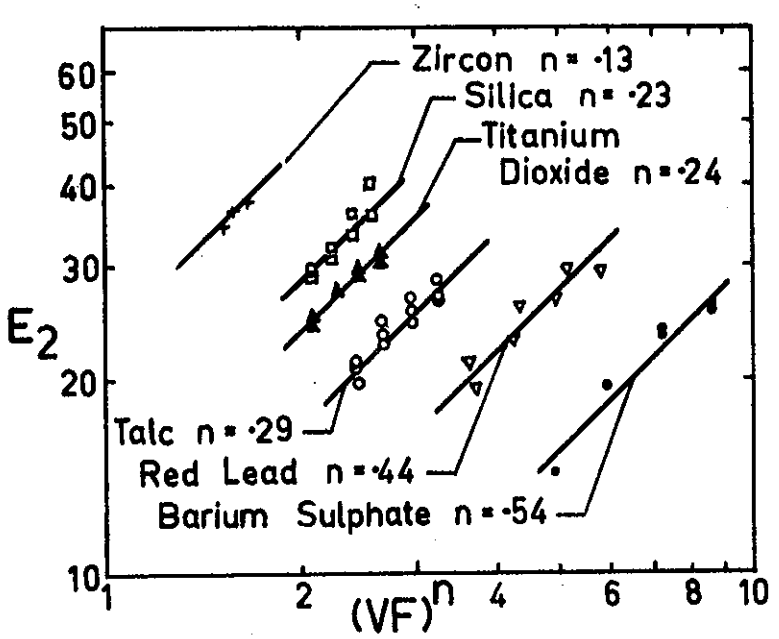

FIG. 6 CONCENTRATION EFFICIENCY vs. $(VF)^n$ FOR $C > C_c$ - CYCLONE I

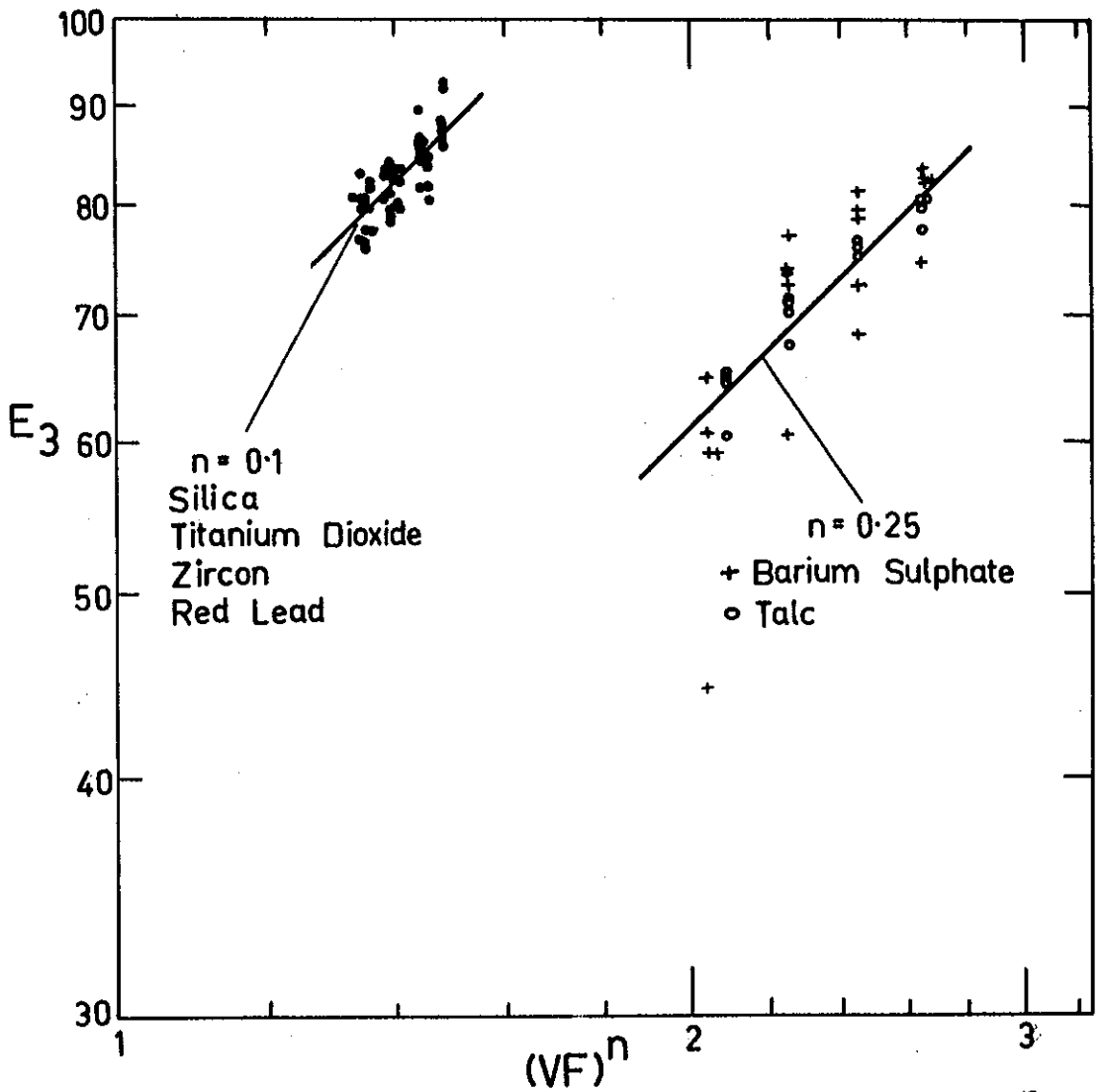

FIG. 7 CLARIFICATION EFFICIENCY vs. $(VF)^n$ FOR $C<C_c$ – CYCLONE I

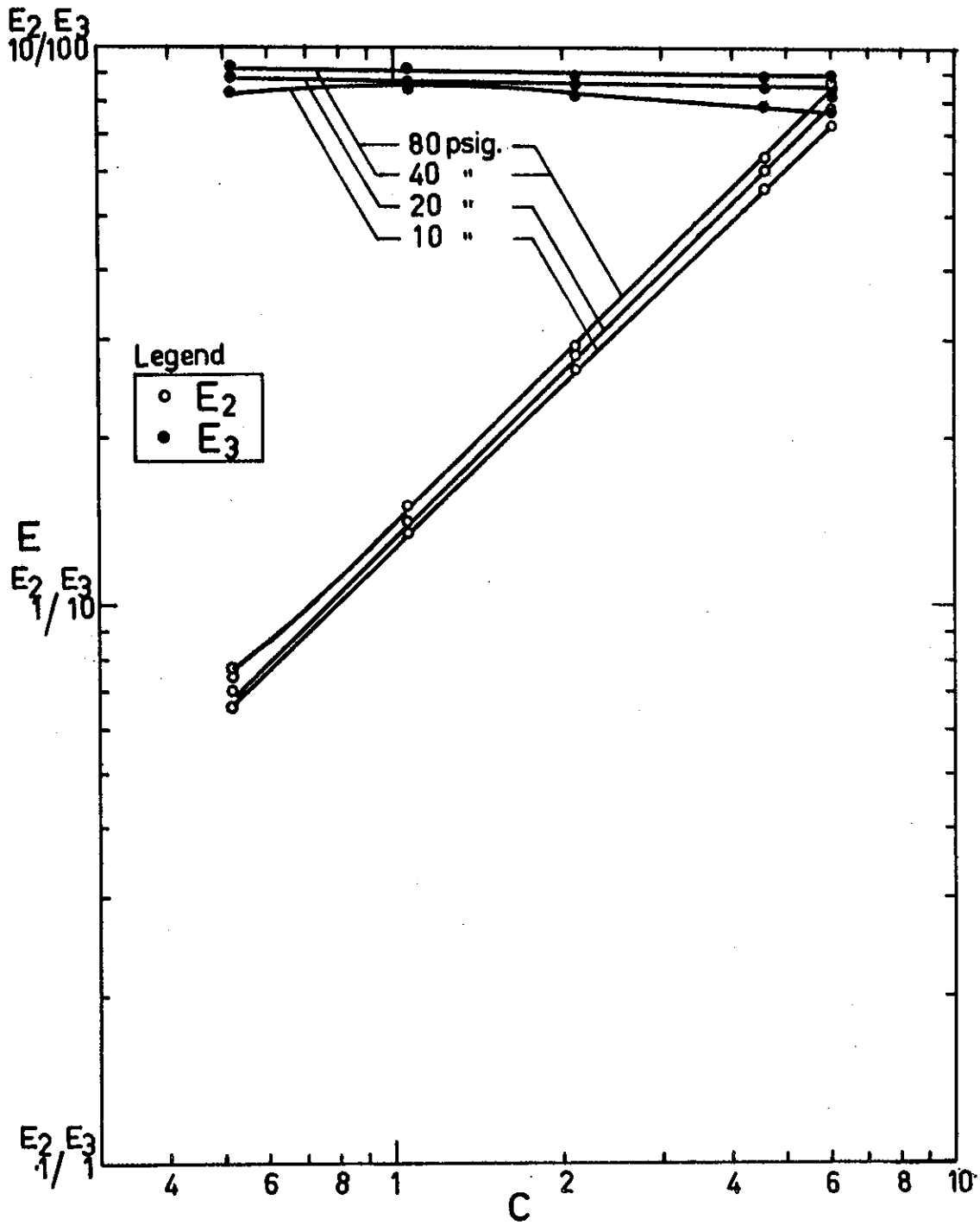

FIG. 8 EFFICIENCY vs. FEED CONCENTRATION FOR TITANIUM DIOXIDE - CYCLONE II

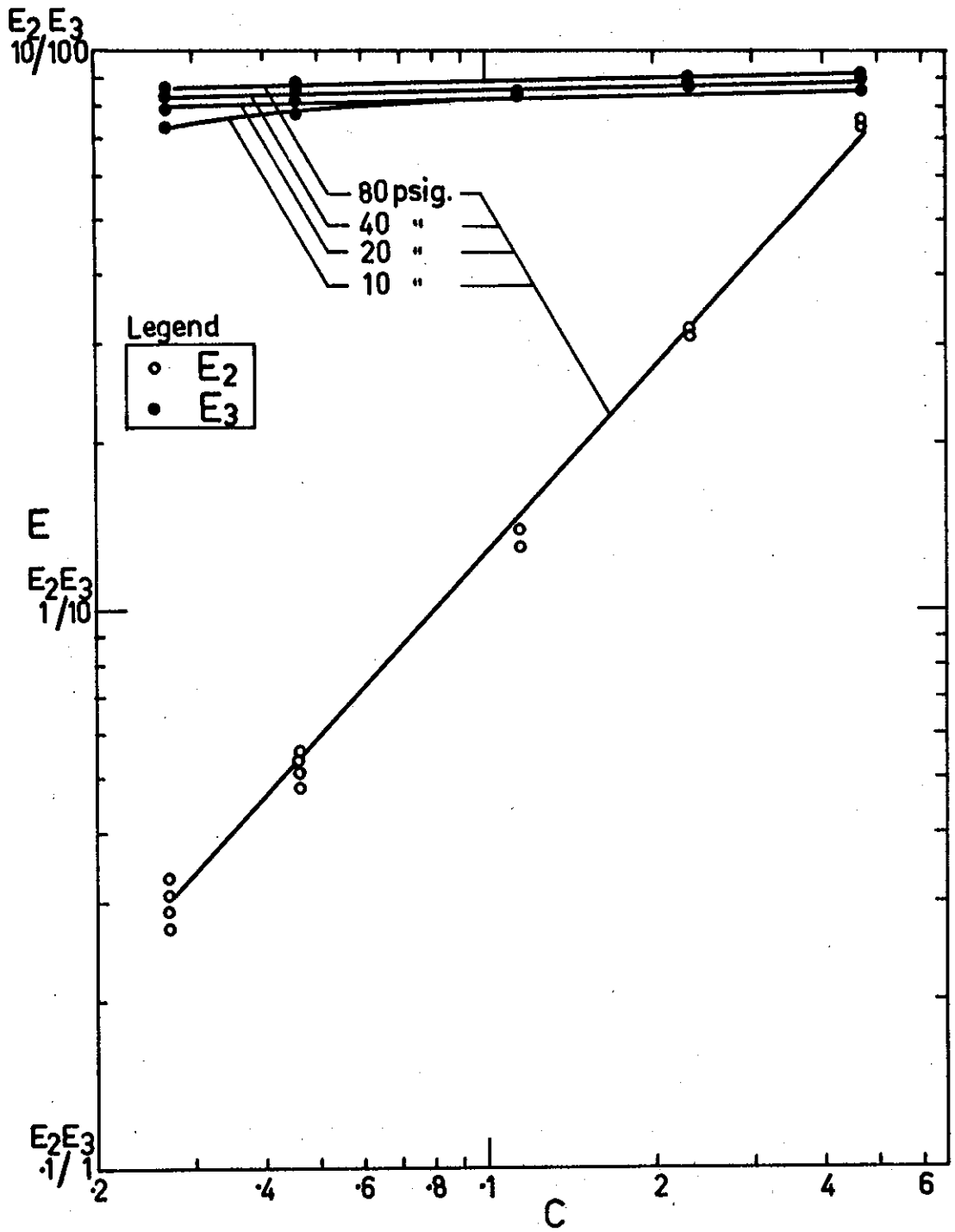

FIG. 9 EFFICIENCY vs. FEED CONCENTRATION FOR RED LEAD — CYCLONE II

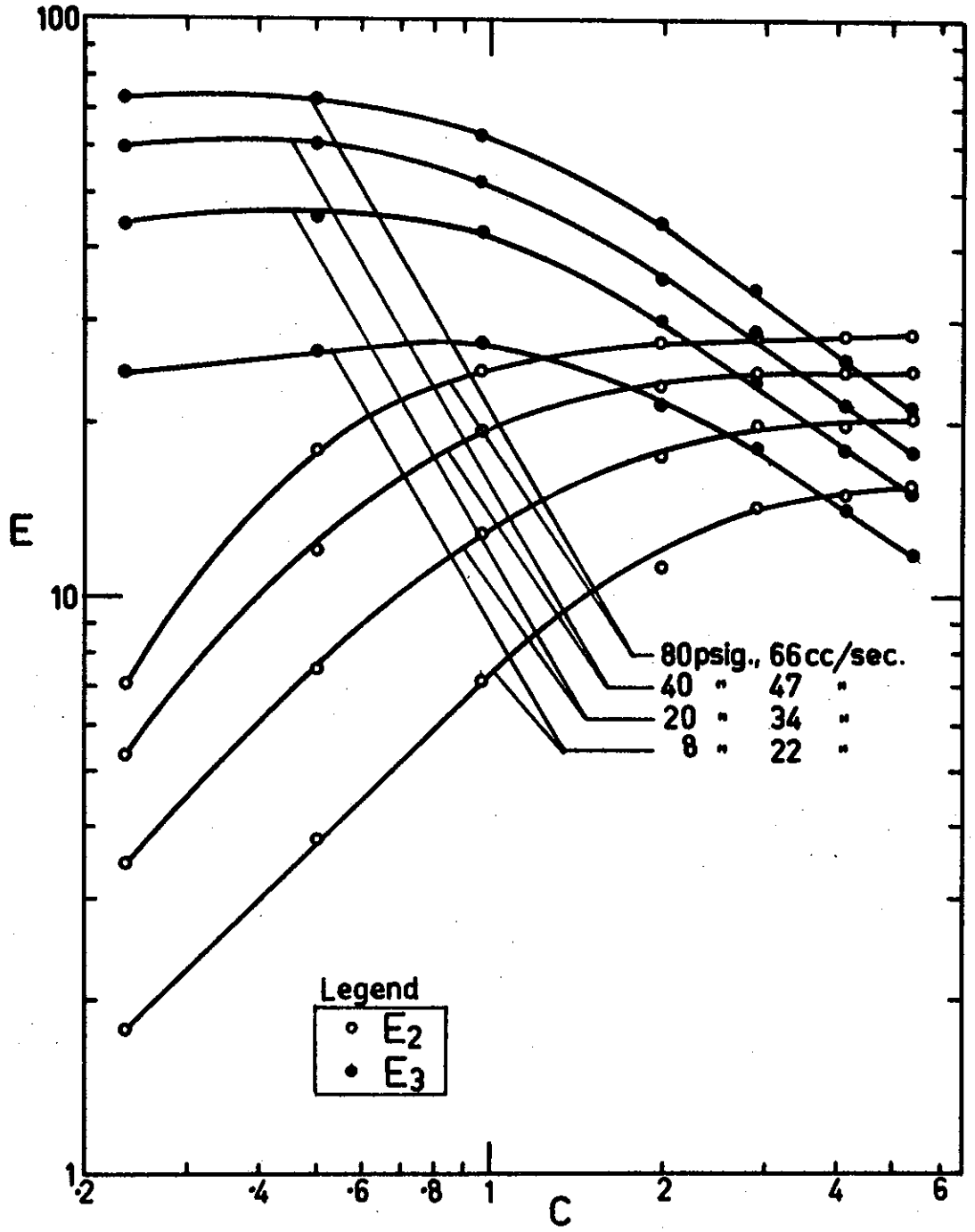

FIG. 10 EFFICIENCY vs. FEED CONCENTRATION FOR BARIUM SULPHATE-CYCLONE III

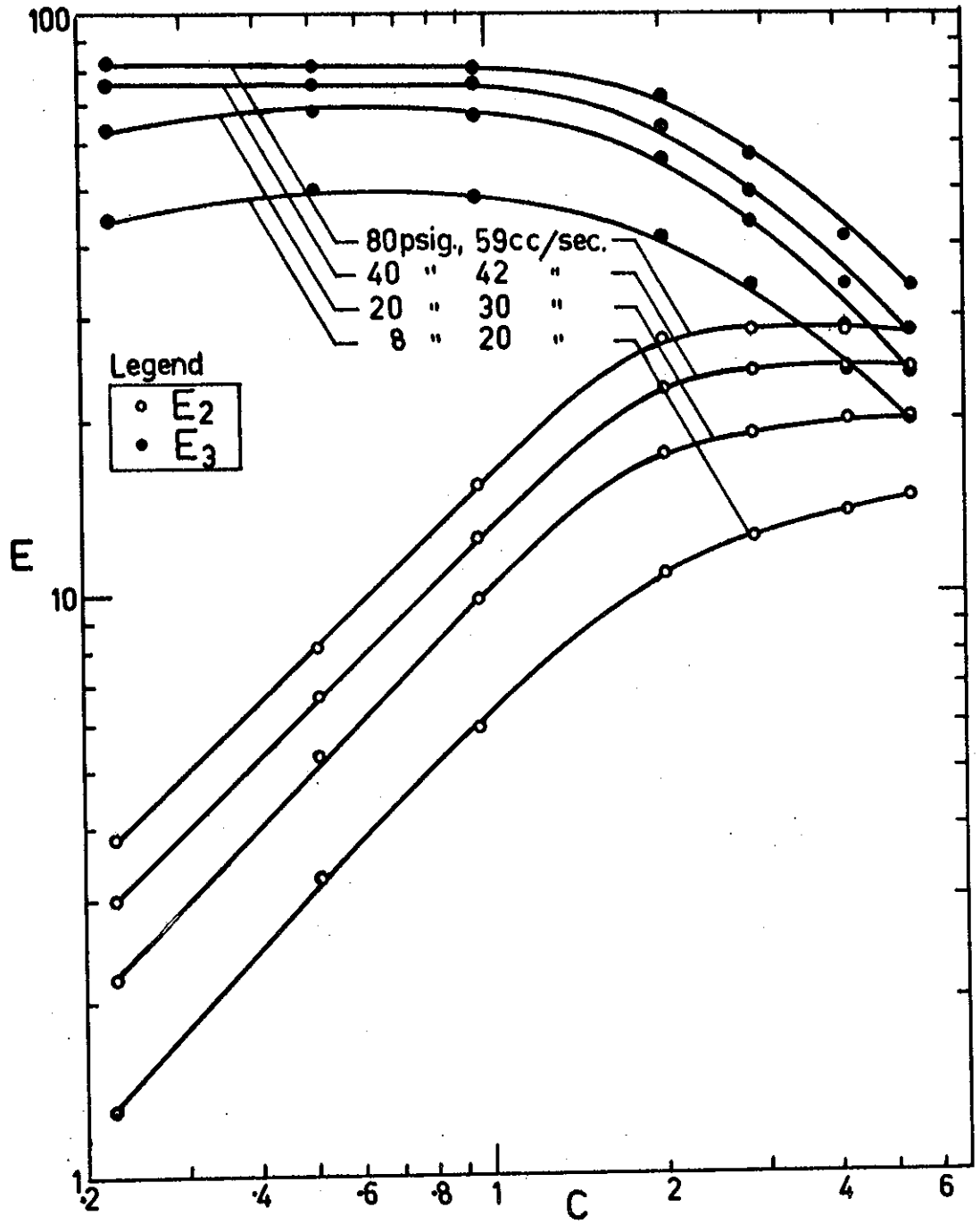

FIG. 11 EFFICIENCY vs. FEED CONCENTRATION FOR BARIUM SULPHATE - CYCLONE IV

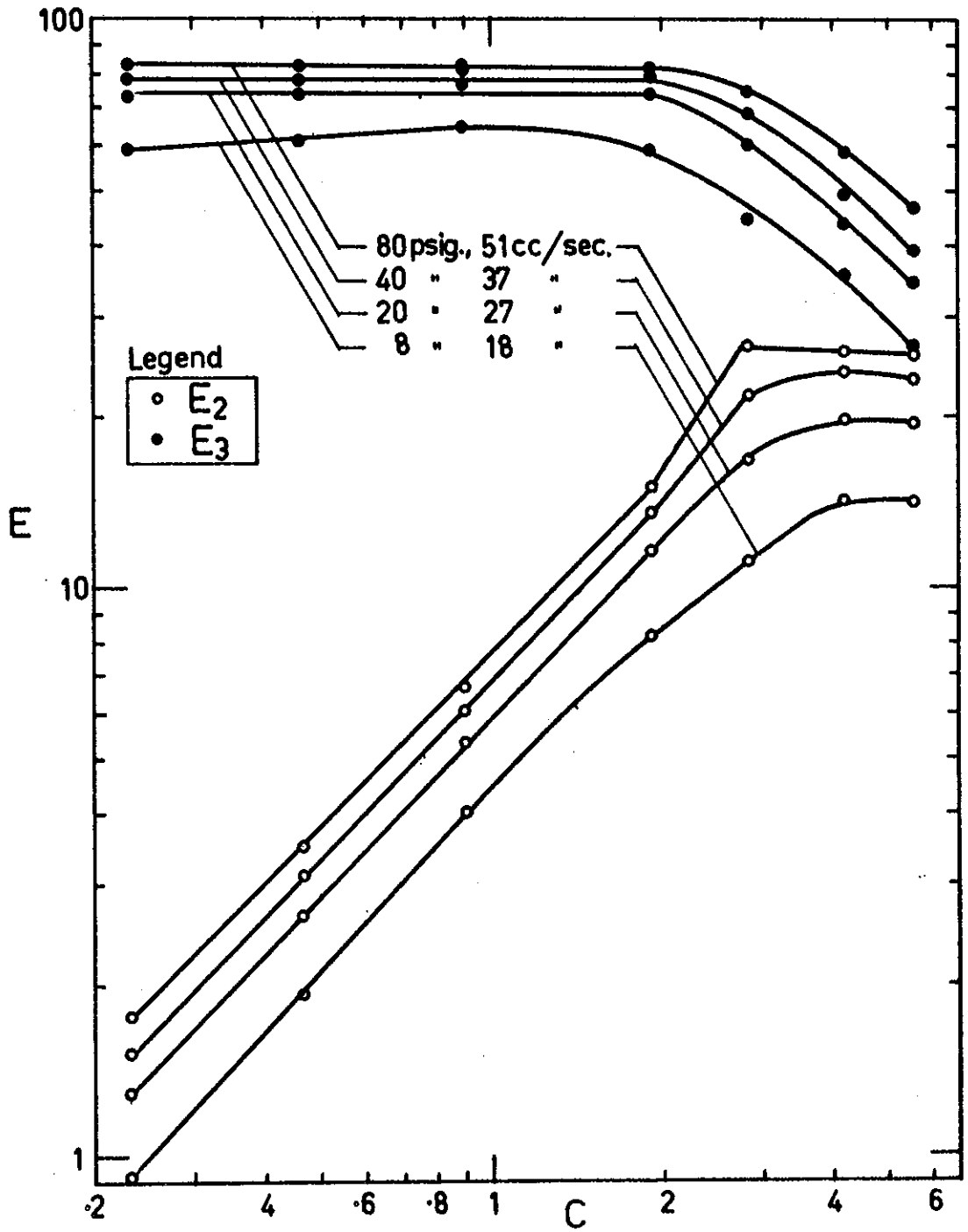

FIG. 12 EFFICIENCY vs. FEED CONCENTRATION FOR BARIUM SULPHATE - CYCLONE I

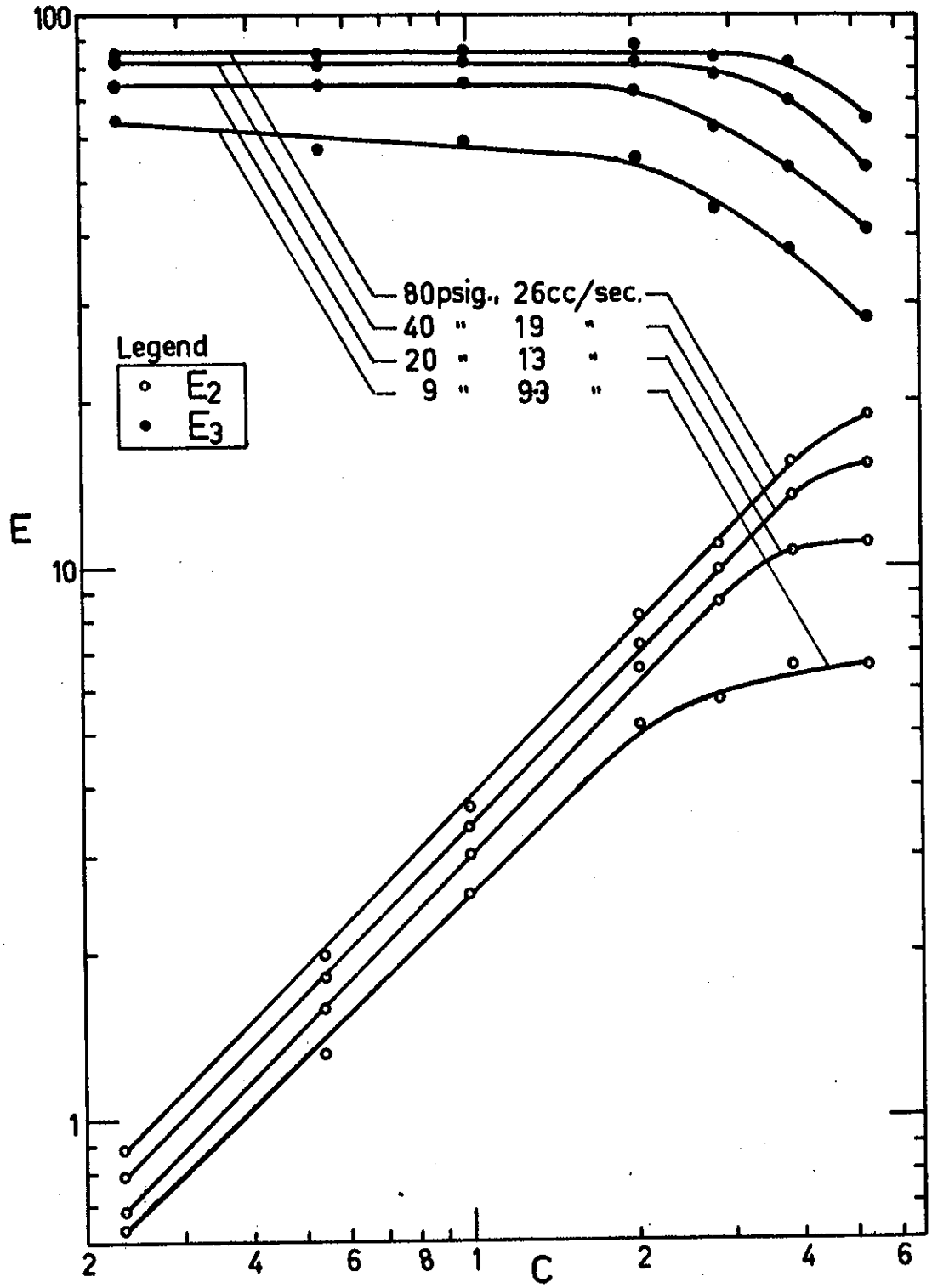

FIG. 13 EFFICIENCY vs. FEED CONCENTRATION FOR BARIUM SULPHATE-CYCLONE V

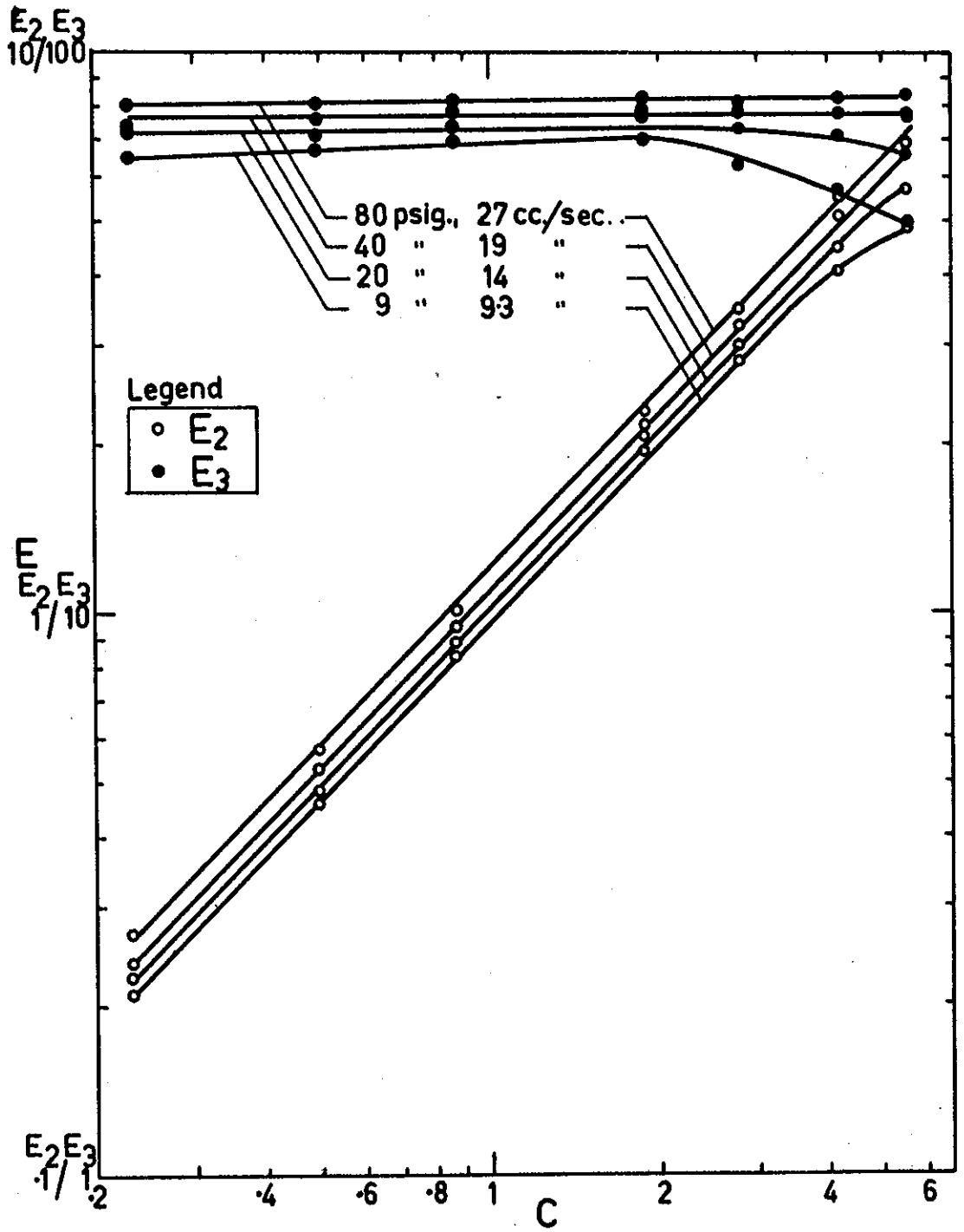

FIG. 14 EFFICIENCY vs. FEED CONCENTRATION FOR BARIUM SULPHATE - CYCLONE II

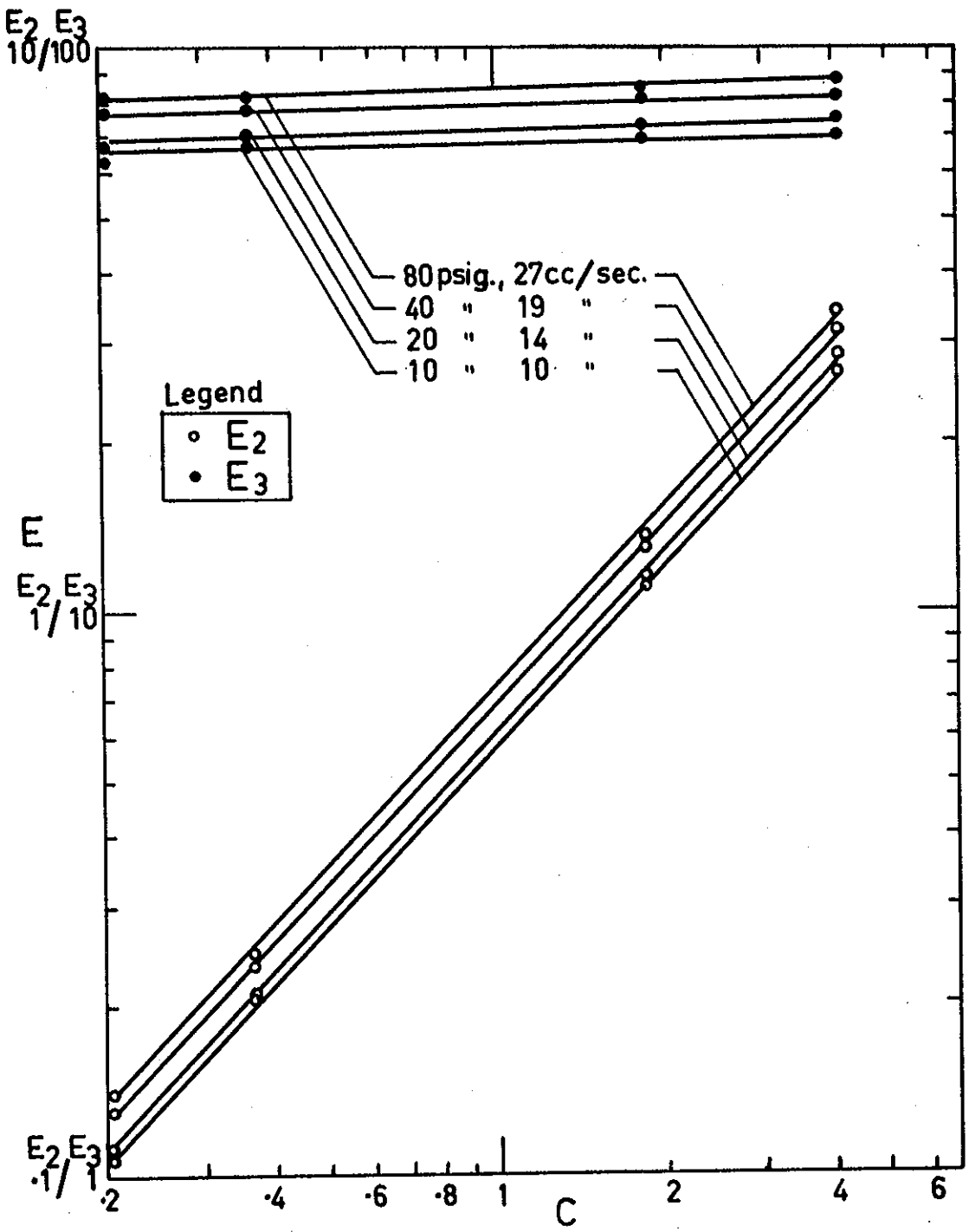

FIG. 15 EFFICIENCY vs. FEED CONCENTRATION FOR BARIUM SULPHATE-CYCLONE VI